Acta Cryst. (1995). **B51**, 182–187

Structure of a Metastable Phase of Piracetam From X-ray Powder Diffraction Using the Atom–Atom Potential Method

BY D. LOUËR AND M. LOUËR

Laboratoire de Cristallochimie, CSIM (URA CNRS 1495), Université de Rennes I, Avenue du Général Leclerc, 35042 Rennes CEDEX, France

V. A. DZYABCHENKO

Karpov Institute of Physical Chemistry, ul. Obukha 10, Moscow 107120, Russia

AND V. AGAFONOV AND R. CEOLIN

Laboratoire de Chimie Physique, Faculté de Pharmacie, 31 avenue de Monge, 37200 Tours CEDEX, France

(*Received* 19 *April* 1993; *accepted* 29 *July* 1994)

Abstract

The crystal structure of the room-temperature metastable phase of 2-oxo-1-pyrrolidineacetamide (piracetam), $C_6H_{10}N_2O_2$, has been solved using the atom–atom potential method and refined by Rietveld refinement from powder diffraction data collected with a curved position-sensitive detector (INEL CPS120) using Debye–Scherrer diffraction geometry with monochromatic X-rays. In the first stage, the indexing of the powder pattern was performed by the successive dichotomy method from data collected with a high-resolution diffractometer using the Bragg–Brentano geometry. The lattice parameters are a = 6.747 (2), b = 13.418 (3), c = 8.090 (2) Å, β = 99.01 (3)°, and the space group is $P2_1/n$. The structure model was obtained from minimization of the crystal-lattice potential energy calculated with semi-empirical atom–atom potentials using the *PMC* [*Packing of Molecules in Crystals*; Dzyabchenko, Belsky & Zorkii (1979). *Kristallografiya*, **24**, 221–226] program. The Rietveld refinement converged to the final crystal-structure model indicator R_B = 0.04 and profile factors R_p = 0.03 and R_{wp} = 0.04. The molecular packing is characterized by intermolecular hydrogen bonds (N—H···O). The structure consists of two types of perpendicular infinite chains of piracetam molecules, which build parallel layers containing rings. No cyclic dimers were found. For a description of the hydrogen-bond patterns, the method based on graph theory was employed.

Introduction

2-Oxo-1-pyrrolidineacetamide (conventional pharmaceutical name piracetam) is used in human therapeutics, particulary in chronic and acute alcoholism with symptoms of delirium, because it acts on the central nervous system. The occurrence of three crystalline polymorphic varieties of piracetam has been proved (Weltscheva-Pavlova, 1979). Forms II and III are prepared by crystallization from solutions in various solvents at room temperature. Both phases transform, at *ca* 400 K, into form I and melting is observed at 435 K. Form I can be obtained at room temperature simply by quenching the stable high-temperature phase. However, it is not stable at 298 K and transforms into form II within a few hours after quenching. Thus, form I is a high-temperature phase with a thermal stability range as narrow as 25–35 K. The crystal structures of forms II (triclinic) and III (monoclinic) have already been determined (Bandoly, Clemente, Grassi & Pappalardo, 1981; Admiraal, Eikelenboom & Vos, 1982; Galdecki & Glowka, 1983). No crystallographic investigation about form I of piracetam has been reported and its crystal structure is unknown.

In recent years a number of crystal structures have been solved *ab initio* from powder diffraction data collected with conventional X-ray sources and using direct or Patterson methods for structure solution. Most of these are inorganic or organometallic systems, not organic molecular systems. With organic materials a problem occurs with the limited quantity of available information contained in the X-ray powder diffraction pattern, as a consequence of the fall off of reflection intensities as 2θ increases. Nevertheless, Lightfoot *et al.* (1993) and Cernik *et al.* (1991) gave several examples chosen especially to demonstrate the use of Patterson, direct, and also maximum entropy methods for determining the structure of organic materials.

A promising advance is the use of the atom–atom potential method (Kitaigorodskii, 1973; Pertsin & Kitaigorodskii, 1987) to obtain crystal structure models for organic solids. This method has already succeeded in the single-crystal structure analysis of organic compounds such as 6,13-pentacenequinone (Dzyabchenko, Zavodnik & Belsky, 1979) and *N*-(4-dimethylamino-

phenyl)phthalimide (Mamedova, Dzyabchenko, Zavodnik & Belskii, 1980).

The present paper deals with an example of the application of the atom–atom potential method in the crystal structure investigation of the room-temperature metastable phase of piracetam (form I) by means of conventional monochromatic X-ray powder diffraction. Due to the metastability of this phase at room temperature, data were collected within 2 h using a position-sensitive detector.

Experimental

Form I of piracetam was obtained from a sample containing a mixture of the triclinic and monoclinic phases. The sample was heated in air at 410 K for 30 min and quenched at room temperature. Two powder diffraction data sets were used for the study.* For indexing and calibration of the position-sensitive detector (PSD) used in one of the diffraction geometries, an accurate powder pattern was obtained with a high-resolution powder diffractometer (Siemens *D*500), using Bragg–Brentano geometry. Pure Cu $K\alpha_1$ radiation (λ = 1.5405981 Å) was produced with an incident-beam curved-crystal germanium monochromator and asymmetric focusing (short focal distance 124 mm, long focal distance 216 mm). The alignment of the diffractometer was checked with standard reference materials (Louër, 1991). The zero error was measured as less than 0.01° (2θ). The instrumental resolution function (IRF) has been described by Louër & Langford (1988). To reduce the effect of transparency of the material, a thin layer of material was deposited on a silicon wafer. The powder diffraction pattern was scanned in steps of 0.02° (2θ) up to 70° and a fixed counting time (17 s) was employed. At the end of data collection, data were again collected in the low angle region. It revealed the presence of a mixture of the room-temperature metastable phase and the triclinic form as a consequence of a slow phase transformation. The precise determination of peak positions was carried out with the Socabim fitting program *PROFILE*, available in the PC software package *DIFFRAC-AT* supplied by Siemens.

Data acquisition for structure analysis was performed with an INEL cylindrical PSD (CPS 120), which allows for simultaneous recording of a powder diffraction pattern over a range of 120°. The detector consists of 4096 channels and the angular step is approximately 0.03° (2θ). It has been used in a Debye–Scherrer geometry operating with monochromatic radiation. Cu $K\alpha_1$ was selected with an incident-beam curved-quartz monochromator with asymmetric focusing (short focal distance 130 mm, long focal distance 510 mm). The geometrical arrangement has been shown elsewhere (Fig.1 in Louër, Louër & Touboul, 1992). The initial sample of piracetam was introduced in a 0.5 mm diameter Lindemann glass capillary. After a thermal treatment at 410 K for half an hour and quenching at room temperature, the capillary was immediatly mounted at the centre of the goniometer circle, of 250 mm radius of curvature. During the experiment the sample was rotated around the θ axis to ensure proper averaging over the crystallites. In order to reduce the effect of non-angular linearity of the PSD, a segmented linear calibration was carried out from the sample itself, as described elsewhere (Louër, Louër & Touboul, 1992). It was based on the peak positions of 52 diffraction lines in the range 10–60° (2θ), measured from the data collected with the high-resolution diffractometer. At angles greater than 57.50°, no reliable diffraction information was obtained for this material.

Data analysis

Powder pattern indexing

Indexing of the powder diffraction pattern of form I was performed on the data collected with the focusing high-resolution diffractometer by the successive dichotomy method (Louër & Louër, 1972), using the PC version of the program *DICVOL*91 (Boultif & Louër, 1991). The first 20 lines were completely indexed on the basis of a monoclinic solution [M_{20} = 22, F_{20} = 45 (0.0133,33)]. Refinement of the cell dimensions from the complete powder diffraction data gave: a = 6.747 (2), b = 13.418 (3), c = 8.090 (2) Å, β = 99.01 (3)°, V = 723.4 (3) Å^3. It was seen that the possible space group was $P2_1/n$ ($0k0$: $k = 2n$, $h0l$: $h + l = 2n$) and the final figures of merit were M_{20} = 25, F_{20} = 49 (0.0145,42).

Structure solution

As reported before, no reliable information is available on the pattern at angles greater than 57.50° (2θ) due to the fall off of reflection intensities with increasing angle. Attempts to find an approximate structure model failed using direct methods. Consequently, a computational study of the piracetam polymorphs based on minimization of the crystal-lattice potential energy, calculated with semi-empirical atom–atom potentials, was used for structure solution.

The geometric parameters (bond distances, valence and torsional angles) of the piracetam molecule in the monoclinic and triclinic crystals already studied are very similar. This led us to expect that the same conformation would occur in the room-temperature metastable monoclinic phase (form I). The packing calculations were made using the *PMC* program (Dzyabchenko, Belsky & Zorkii, 1979) with a set of atom–atom potentials

* A list of structure factors has been deposited with the IUCr (Reference HA0135). Copies may be obtained through the Managing Editor, International Union of Crystallography, 5 Abbey Square, Chester CH1 2HU, England.

Table 1. *Crystallographic data and details of the Rietveld refinement for* $C_6H_{10}N_2O_2$

Crystal name	Piracetam, 2-oxo-1-pyrrolidineacetamide
Formula weight (g)	142.2
Crystal symmetry	Monoclinic
Space group	$P2_1/n$
Z	4
D_x (g cm^{-3})	1.306
Wavelength (Å)	1.540598
Step increment, 2θ (°)	0.03
Number of reflections	186
Number of profile parameters	11
Number of non-H atoms	10
Number of H atoms	10
$R_B = \sum\|I(\text{obs}) - I(\text{calc})\| / \sum I(\text{obs})$	0.04
$R_p = \sum\|y_i(\text{obs}) - (1/c)y_i(\text{calc})\| / \sum y_i(\text{obs})$	0.03
$R_{wp} = (\sum w_i\|y_i(\text{obs}) - (1/c)y_i(\text{calc})\|^2 / \sum w_i[y_i(\text{obs})]^2)^{1/2}$	0.04

Table 2. *Atomic coordinates with e.s.d.'s in parentheses**

	x	y	z
C(1)	0.067 (2)	0.478 (1)	0.237 (2)
C(2)	0.271 (2)	0.513 (1)	0.325 (1)
C(3)	0.413 (2)	0.447 (1)	0.238 (2)
C(4)	0.289 (2)	0.362 (1)	0.146 (1)
C(5)	−0.090 (2)	0.343 (1)	0.068 (1)
C(6)	−0.135 (2)	0.249 (1)	0.170 (1)
N(1)	0.084 (2)	0.392 (1)	0.148 (1)
N(2)	−0.289 (1)	0.200 (1)	0.101 (1)
O(1)	−0.106 (1)	0.510 (1)	0.257 (1)
O(2)	−0.021 (1)	0.220 (1)	0.299 (1)
H(21)	0.279	0.585	0.297
H(22)	0.271	0.494	0.446
H(31)	0.467	0.492	0.164
H(32)	0.513	0.424	0.333
H(41)	0.324	0.362	0.033
H(42)	0.337	0.299	0.212
H(51)	−0.220	0.377	0.028
H(52)	−0.053	0.302	−0.048
H(211)	−0.296	0.201	−0.040
H(221)	−0.273	0.128	0.144

* Overall isotropic atom displacement parameters $U = 0.070$ Å^2.

Table 3. *Distances* (Å) *and angles* (°) *with e.s.d.'s in parentheses*

C(1)—C(2)	1.52 (2)	C(2)—C(1)—N(1)	111 (2)
C(1)—N(1)	1.37 (2)	C(2)—C(1)—O(1)	128 (3)
C(1)—O(1)	1.27 (2)	N(1)—C(1)—O(1)	120 (2)
C(2)—C(3)	1.55 (2)	C(1)—C(2)—C(3)	101 (1)
C(3)—C(4)	1.54 (2)	C(2)—C(3)—C(4)	108 (2)
C(4)—N(1)	1.45 (2)	C(3)—C(4)—N(1)	103 (2)
C(5)—C(6)	1.57 (2)	C(6)—C(5)—N(1)	110 (2)
C(5)—N(1)	1.41 (2)		
C(6)—N(2)	1.28 (2)	C(5)—C(6)—N(2)	113 (2)
C(6)—O(2)	1.25 (1)	C(5)—C(6)—O(2)	123 (2)
		N(2)—C(6)—O(2)	124 (2)
Hydrogen bonds			
N(2)···O(2^{i})	2.90 (1)		
N(2)···O(1^{ii})	2.93 (1)		

Symmetry codes: (i) $x - \frac{1}{2}, \frac{1}{2} - y, z - \frac{1}{2}$; (ii) $-\frac{1}{2} - x, y - \frac{1}{2}, \frac{1}{2} - z$.

from Momany, Carruthers, McGuire & Scheraga (1974) and atom charges calculated by the CNDO/2 method. The *PMC* program utilizes an advanced version of the convergence procedure (Williams, 1971) to calculate crystal-lattice potential sums. Due to the convergence acceleration of this version, the computational time needed to calculate the lattice energy is reduced by a factor of ten. The energy minimization was made within the experimentally found space group $P2_1/n$, and with fixed lattice parameters. The three translation and three rotation parameters φ, θ, ψ (the Eulerian angles which describe the orientation of the molecule occupying the symmetry position 1) were allowed to vary, while the symmetry-related molecules moved in a dependent way. The Eulerian angles φ and θ were varied within 180° and ψ was varied within 360°. The grid increments were taken as 1/10 of the corresponding edge length for molecular translations, and 30° for the three rotations. The monoclinic cell angle β (99.12°) is not greatly different from rectangular. This made it possible to provisionally introduce some extra parameter space symmetry, thus reducing the range of starting rotations twice (equivalent to assuming the *Pmmm* Cheshire symmetry with a corresponding contraction of the asymmetric region). At the final step of the global search, the extra symmetry was eliminated by optimizing the additional starting points obtained by changing the cell angle β to $180 - \beta$ for each successfully optimized structure. The minima found were inspected for the occurrence of identical solutions, including the symmetry-related ones (Hirsheld, 1968; Dzyabchenko, 1983). The local minimum search was made using the variable-metric method (Fletcher, 1972), which realizes the quasi-Newton algorithm with analytical first derivatives. As a result of packing calculations, two distinct minima with E_r = −100.78 and −87.29 kJ mol^{-1} were found. Only the highest energy structure (E_r = −87.29 kJ mol^{-1}) was correct, as shown by the Rietveld refinement, in agreement with the metastability of this form. For comparison, the minima calculated for the other crystal forms of piracetam were found as follows: E_r = −99.44 kJ mol^{-1} for the triclinic structure (form II) and E_r = −97.30 kJ mol^{-1} for the monoclinic structure (form III).

Structure refinement

The atomic coordinates of the model obtained by the atom–atom potential method were input in the Rietveld refinement program *FULLPROF* (Rodriguez-Carvajal, 1990), using the data set collected with the PSD limited to the range 12–57.51° (2θ; 186 independent reflections). A pseudo-Voigt function was selected to describe individual line profiles, with a possible variation of the shape parameter η. In order to describe the angular dependence of FWHM values, the usual quadratic form in $\tan\theta$ was used. The following parameters were included in the Rietveld refinement: 30 atomic coordinates of non-H

atoms, 1 scale factor, 1 overall U parameter, 1 zero-point, 4 unit-cell parameters, 3 FWHM and 1 line asymmetry factor, and 2 parameters to describe the angular dependence of the pseudo-Voigt shape factor. As already observed in a previous work (Louër *et al.*, 1992), the representation of the background by a polynomial was not found satisfactory in the initial part of the pattern; consequently, a description of the background by linear interpolation between 20 given points was preferred in the final least-squares refinement. At this stage, the H-atom positions were calculated; they were introduced in the last calculation, but not refined, resulting in an improvement of the R_B factor from 0.06 to 0.04. The details of the refinement are gathered in Table 1. Fig. 1 shows the final fit between calculated and observed patterns. It corresponds to satisfactory crystal-structure model indicator, $R_B = 0.04$, and profile factors, $R_p = 0.03$ and $R_{wp} = 0.04$. The low value of the profile indicators is a consequence of the high background observed with diffraction data collected with the PSD (for a discussion, see Eriksson, Louër & Werner, 1989). Final atomic parameters are given in Table 2 and selected interatomic

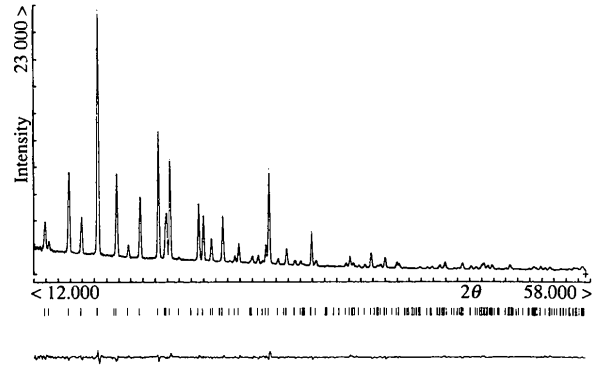

Fig. 1. Final Rietveld difference plot of room-temperature metastable form I of piracetam from the INEL CPS120 diffraction data set.

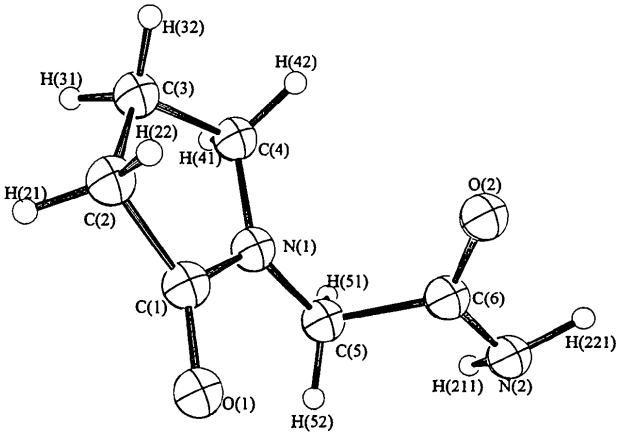

Fig. 2. The piracetam molecule with atom numbering.

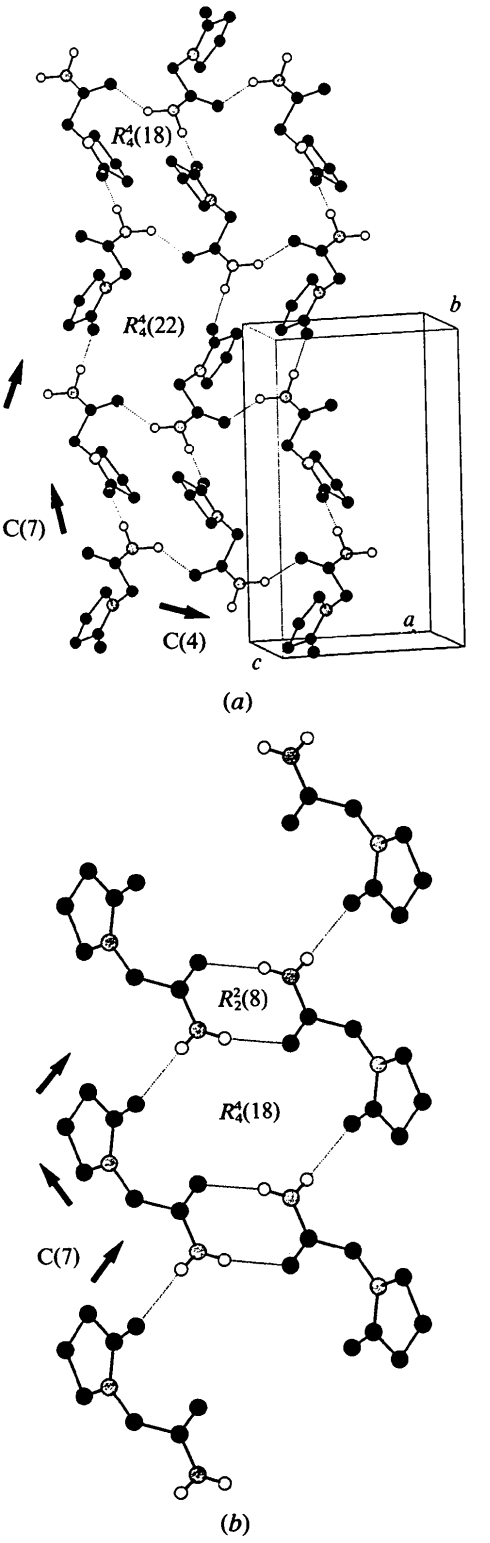

Fig. 3. (*a*) View of piracetam molecules and hydrogen-bond motifs in the crystal of form I; (*b*) hydrogen-bond motifs in the crystal of forms II and III. Small lines represent hydrogen bonds; for clarity, only the H atoms bound to N(2) are represented here. Arrows indicate the direction of the chains C(4) and C(7).

distances and angles in Table 3. Fig. 2 presents the *ORTEX* (McArdle, 1993) molecular structure and atomic numbering of piracetam. A *MOLDRAW* (Cense, 1989) view of all molecules, as packed into the unit cell, is shown in Fig. 3(*a*).

Results and discussion

Experimental bond lengths and angles of the pyrrolidone ring are similar to those observed in forms II and III within observed standard deviations. The conformation of the pyrrolidone ring is similar to those in the stable forms, but the conformation of the acetamide group is slightly different. Thus, the torsional angles N(1)—C(5)—C(6)—N(2) and N(1)—C(5)—C(6)—O(2) are equal to 178 (1) and 4.2 (16)°, respectively, while the corresponding values are equal to 155.2 and 27.1° in the triclinic form II, and 159.2 and 23.3° in the monoclinic form III. These differences may be caused, on the one hand, by the possibility of 'free rotation' about the C(5)—C(6) bond and, on the other hand, by the capability of N(2) and O(2) atoms to form hydrogen bonds. The molecular packing of form I of piracetam is characterized by two classical intermolecular hydrogen bonds, as suggested by the two N—O distances N(2)···O(2^{i}) = 2.90 (1) and N(2)···O(1^{ii}) = 2.93 (1) Å (see Table 3). For a description of hydrogen-bond patterns, the method based on graph theory was employed (Etter, MacDonald & Bernstein, 1990; Etter, 1990). The graph sets are assigned first to motifs, and then to networks. The motif (containing hydrogen as well as covalent bonds) is described by graph sets which are specified using the pattern designator (*G*), its degree (*r*), and the number of donors (*d*) and acceptors (*a*): $G_d^a(r)$, where *G* is one of the following letters: *C* (infinite chain), *D* (definite chain), *R* (ring) or *S* (intramolecular ring). The parameter *r* represents the number of atoms in the ring or the repeat length of a chain. After the assignment of graph sets, the total hydrogen-bonded network, N_1 (primary) and N_2 (secondary), is stated as a series of graph sets.

The N(2)—H···O(2^{i}) and N(2)—H···O(1^{ii}) hydrogen bonds link the piracetam molecules into two types of perpendicular infinite chains, C(4) and C(7), which form parallel layers containing secondary rings R_4^4 (18) and R_4^4 (22) [Fig. 3(*a*)]. No cyclic dimers were found, although cyclic dimers are the usual hydrogen-bond motifs of amides (Leiserowitz & Schmidt, 1969). The layers are related by van der Waals' interactions. The hydrogen-bond network for form I is the following: N_1 = C(4)C(7), $N_2 = R_4^4$ (18)R_4^4 (22).

For comparison, the triclinic (form II) and monoclinic (form III) structures of piracetam present the same motif of hydrogen bonds, which is different from that of the room-temperature metastable form I [Fig 3(*b*)]. This motif includes two rings and one infinite chain, C(7). The primary ring R_2^2 (8) is formed by cyclic dimerization of two acetamide groups about the centre of inversion, and the secondary ring R_4^4 (18) is a product of hydrogen-bond interactions between acetamide–acetamide and acetamide–pyrrolidone groups. The rings and the chains build infinite ribbons related by van der Waals' interactions. The network for the two stable forms is the following: N_1 = C(7)R_2^2 (8), $N_2 = R_4^4$ (18). Note that the packing of ribbons in the triclinic structure (form II) is different from that in the monoclinic structure (form III).

Concluding remarks

We have demonstrated that a 'pure' organic crystal structure having only a few hours of life can be solved by the generation of a model, using the atom–atom potential method, and refined using data collected at room-temperature on a laboratory-based diffractometer. The structure solution of the room-temperature metastable form of piracetam gives new results, of interest from a pharmaceutical and crystallo-chemical point of view. It should be noted that the limitation of available diffraction data to $\sin\theta/\lambda = 0.31$ Å^{-1} is a source of inaccuracy of atomic coordinates and, therefore, of abnormality of some bond distances discussed above. (The number of refined structure parameters is 30 for a number of 186 *hkl* reflections.) Nevertheless, they are precise enough to satisfactorily describe the molecular geometry and packing arrangement of the metastable monoclinic phase of piracetam. In addition, the quality of the final Rietveld plot attests the validity of the structure model derived from the atom–atom potential method used for structure solution.

The authors acknowledge Dr F. Lambert from ISOCHEM (Gennevilliers) who kindly provided them with the piracetam powder.

References

ADMIRAAL, G., EIKELENBOOM, J. C. & VOS, A. (1982). *Acta Cryst.* B**38**, 2600–2605.

BANDOLY, G., CLEMENTE, D. A., GRASSI, A. & PAPPALARDO, G. C. (1981). *Mol. Pharmacol.* **20**, 558–564.

BOULTIF, A. & LOUËR, D. (1991). *J. Appl. Cryst.* **24**, 987–993.

CENSE, J. M. (1989). *Tetrahedron Comput. Methodol.* **2**, 65–71.

CERNIK, R. J., CHEETHAM, A. K., PROUT, C. K., WATKIN, A. P., WILKINSON, A. P. & WILLIS, B. T. M. (1991). *J. Appl. Cryst.* **24**, 222–226.

DZYABCHENKO, A. V. (1983). *Acta Cryst.* A**39**, 941–946.

DZYABCHENKO, A. V., BELSKY, V. K. & ZORKII, P. M. (1979). *Kristallografiya*, **24**, 221–226.

DZYABCHENKO, A. V., ZAVODNIK, V. E. & BELSKY, V. K. (1979). *Acta Cryst.* B**35**, 2250–2253.

ERIKSSON, L., LOUËR, D. & WERNER, P.-E. (1989). *J. Solid State Chem.* **81**, 9–20.

ETTER, M. C. (1990). *Acc. Chem. Res.* **23**, 120–126.

ETTER, M. C., MACDONALD, J. C. & BERNSTEIN, J. (1990). *Acta Cryst.* B**46**, 256–262.

FLETCHER, R. (1972). *Fortran Subroutines for Minimization by Quasi-Newton.* Theoretical Physics Division, Harwell, Berkshire, Atomic Energy Research Establishment, AERE-R7125.
GALDECKI, Z. & GLOWKA, M. L. (1983). *Pol. J. Chem.* **57**, 1307–1312.
HIRSHELD, F. L. (1968). *Acta Cryst.* A**24**, 301–311.
KITAIGORODSKII, A. I. (1973). *Molecular Crystals and Molecules.* New York, London: Academic Press.
LEISEROWITZ, L. & SCHMIDT, G. M. J. (1969). *J. Chem. Soc. A*, pp. 2372–2382.
LIGHTFOOT, P., TREMAYNE, M. J., HARRIS, K. D. M., GLIDEWELL, C., SHANKLAND, K., GILMORE, C. J. & BRUCE, P. G. (1993). *Mater. Sci. Forum*, **133–136**, 207–212.
LOUËR, D. (1991). *Mater. Sci. Forum*, **79–82**, 17–26.
LOUËR, D. & LANGFORD, J. I. (1988). *J. Appl. Cryst.* **21**, 430–437.
LOUËR, D. & LOUËR, M. (1972). *J. Appl. Cryst.* **5**, 271–275.
LOUËR, D., LOUËR, M. & TOUBOUL, M. (1992). *J. Appl. Cryst.* **25**, 617–623.
MAMEDOVA, N. S., DZYABCHENKO, A. V., ZAVODNIK, V. E. & BELSKII, V. K. (1980). *Cryst. Struct. Comm.* **9**, 713–715.
MCARDLE, P. J. (1993). *J. Appl. Cryst.* **26**, 752.
MOMANY, F. A., CARRUTHERS, L. M., MCGUIRE, R. F. & SCHERAGA, H. A. (1974). *J. Phys. Chem.* **78**, 1598–1619.
PERTSIN, A. J. & KITAIGORODSKII, A. I. (1987). *The Atom–Atom Potential Method.* Berlin: Springer.
RODRIGUEZ-CARVAJAL, J. (1990). In Collected Abstracts of Powder Diffraction Meeting. Toulouse, France, July 1990, p.127.
WELTSCHEVA-PAVLOVA, A. (1979). *Pharmazie*, **34**, 449–450.
WILLIAMS, D. E. (1971). *Acta Cryst.* A**27**, 452–455.

Acta Cryst. (1995). B**51**, 187–197

The Fourfold Disordered Structures of *p*-Chloro-*N*-(*p*-methylbenzylidene)aniline and *p*-Methyl-*N*-(*p*-chlorobenzylidene)aniline

BY KENNETH J. HALLER

Petroleum and Petrochemical College, Chulalongkorn University, Phya Thai Road, Bangkok 10330, *Thailand*

AND A. DAVID RAE,* AIDAN P. HEERDEGEN, DAVID C. R. HOCKLESS AND T. RICHARD WELBERRY

Research School of Chemistry, Australian National University, Canberra, ACT 0200, *Australia*

(*Received* 9 *June* 1994; *accepted* 19 *September* 1994)

Abstract

p-Chloro-*N*-(*p*-methylbenzylidene)aniline, MeCl, and *p*-methyl-*N*-(*p*-chlorobenzylidene)aniline, ClMe, are isostructural, both $C_{14}H_{12}ClN$, M_r = 229.6, differing only in the disposition of a —CH=N— linkage joining two phenyl-ring systems, one with a *p*-Cl atom attached, the other with a *p*-methyl group attached. A non-disordered prototype structure would have the space group $P2_1/n$, Z = 4. MeCl: a = 5.965 (2), b = 7.423 (3), c = 27.420 (3) Å, β = 99.22 (1)°, V = 1198 (1) Å^3, D_x = 1.28 Mg m^{-3}, T = 295 K, μ = 24.5 cm^{-1}, Cu $K\alpha$, λ = 1.5418 Å; ClMe: a = 5.971 (2), b = 7.411 (3), c = 27.462 (3) Å, β = 99.13 (1)°, V = 1200 (1) Å^3, D_x = 1.27 Mg m^{-3}, T = 295 K, μ = 24.3 cm^{-1}, Cu $K\alpha$, λ = 1.5418 Å. The molecules have pseudo-*mmm* symmetry, but no real symmetry. Four pseudo-equivalent orientations occur in the disordered structure. If inversion-related orientations are equally populated, then l odd data are unobserved and the average disordered structure has the space group $P2_1/a$, with $\mathbf{a}' = \mathbf{a}$, $\mathbf{b}' = \mathbf{b}$, $\mathbf{c}' = \mathbf{c}/2$, Z = 2. This was the case for the ClMe crystal studied, but not for MeCl. For the crystals studied, occupation ratios for the reference-, inversion-, mirror- and twofold rotation-related orientations were 0.543:0.189 (3):0.095 (3):0.173 (3) for MeCl and 0.351:0.351:0.149:0.149 (3) for ClMe. A 91-variable model (with 7 degrees of freedom restrained) was used in the constrained refinement of MeCl to refine 660 from 1784 reflections in one quadrant with $I(\mathbf{h}) > 3\sigma[I(\mathbf{h})]$. Final values for $R_1 = \sum_{\mathbf{h}}|\Delta F(\mathbf{h})|/\sum_{\mathbf{h}}|F_o(\mathbf{h})|$ were 0.049 for the 529 l even data, 0.079 for the 131 l odd data, and 0.052 overall. An 87-variable model (with 8 degrees of freedom restrained) was used in the constrained refinement of ClMe to refine 1387 from 2284 unmerged data with $I(\mathbf{h}) > 3\sigma[I(\mathbf{h})]$ to a value for R_1 of 0.044.

Introduction

The disorder in the structures of *p*-chloro-*N*-(*p*-methylbenzylidene)aniline, hereafter referred to as MeCl, and *p*-methyl-*N*-(*p*-chlorobenzylidene)aniline, hereafter referred to as ClMe, was first reported by Bar & Bernstein (1983), but little attempt was made at accurate refinement. We have a long-term interest in diffuse scattering from disordered crystal systems and are particularly interested in the distributions of local structure environments in disordered systems. We have already published some preliminary investigations of the diffuse scattering from MeCl (Welberry, Butler & Heerdegen, 1993; Welberry & Butler, 1994) and work is progressing on ClMe. To further our understanding we considered it useful to obtain a better description of the average cell contents of MeCl and ClMe, as obtained

* Author to whom correspondence should be addressed.